2016

Developing a Relationship between Fermi Diversion Levels of Organic Substrates and Contact Success of Multiwalled Carbon Nanotubes

PHYSICS RESEARCH PROJECT

Table of Contents

Abstract

Carbon nanotubes, with their perfectly symmetrical geometry with delocalized electrons, are known to be excellent conductors of both electrons and phonons (thermal energy). Such arrays are being applied to various applications including the heat dissipation of computer processors. However, much of this conductivity is lost because carbon nanotubes cannot inherently bond with a mating surface covalently. Last year, it was determined that only through oxygen plasma etching, and the introduction of a symmetrically bonded substrate as a juncture between the oxidized bonds of the carbon nanotubes and mating surface, in that case an aluminum plate, would increase the thermal dissipation of nanotubes due to a high contact success of 0.73.

However, the full story is not recognized from this research, as such substrates are extremely expensive to manufacture. **The purpose of this research is to determine and develop a relationship between the fermi levels of organic substrates, all of which are used in the adhesive industry, and the contact success that the substrates enable between Multiwalled carbon nanotubes and metallic mating surfaces.**

Three chemicals (aminopropyl triethoxysilane, hydroxylsilane hydrochloride, and methyl-2-silicoacrylade) were applied to a plasma-etched CNT array and temperature gradients between the top of the resulting juncture and the heat source were calculated. The fermi level of each chemical was also calculated based on the fermi energy of the bonds. The relationship had a positive correlation between Fermi diversion and contact success, but the actual relationship was close (0.98 correlation coefficient) to the following equation:

$$y = \frac{\sqrt{3}}{2} e^{x-12} + \left(1 - \frac{\sqrt{3}}{2}\right) \quad (1)$$

Equation 1, the developed relationship, is consistent with the initial hypothesis of an exponential curve based on 5-space phonon vector theory, but the added coefficients are likely attributed to both symmetricity ratios and phonon transport without any adhesive forces.

In conclusion, the relationship between Fermi level and contact success is given by an exponential expression, with sharply diminishing contact success (conductivity) with a slight decrease in symmetricity from perfectly equilateral geometry.

Introduction

Practical Problems with CPU Dissipation

Computers are used in daily lives more and more frequently and more usefully. Thus, their performance is becoming more of an issue today than it ever has before. Costumers are constantly on the lookout to find the fastest, yet most portable computer on the market.

In its most generic form, a computer processor is the electronic circuitry in a computer that carries out basic computational functions. This is trough millions of flip-flop circuits run through binary code that pass pulses of electric current through transistors, or the junctions that control the direction of the flow of electricity. Unfortunately, each of these junctions produces internal resistance in that the electrical current is "forced" into an unnatural direction. When this amount of resistance is multiplied by the number of transistors found in a typical processor (today upwards of 1 billion transistors), an immense amount of thermal energy is generated by the processor. Too much thermal energy can cause melting of these transistors over time, degrading the processor's performance and even causing permanent damage.

To make matters worse, the frequency of the electrical pulses that are sent through the processor is directly proportional to the actual performance of the chip, with all other factors being equal. While the clock speed can be manually set higher, the rate of induced heat will increase, thus drastically increasing the amount of heat generated by the CPU.

The aforementioned causes are why processor speeds in desktops have capped out at approximately 3.5 GHz over the last seven years. It is important to note that today's trend is towards mobile devices, such as laptops and tablets. Most laptops have a clock speed of below 2.8GHz and most mobile devices have a CPU clock speed below 2.3 GHz. This is due to their smaller form factor, which limits the capability of the cooling components, such as the fan and heatsinks. While many enthusiast desktops have features such as liquid cooling, such systems are a bane to space for other components, and, more importantly, are a chore to maintain. Moreover, such systems are not applicable to other types of computers, particularly those in a slim form factor (laptop, tablet).

Another method currently being developed to bypass this problem involves the use of multi-core processors. This trend has started in 2004 and enables two processor chips on one dye, each performing the same tasks that would otherwise be performed by an individual CPU. However, while the performance to heat ratio is noticeable higher in multi-core CPUs, it is important to note that a 2x performance boost is not possible with a controlled cooling system when compared to a single core CPU.

Therefore, the most efficient way to increase CPU performance remains to increase clock speed.

Unfortunately, the rate of processor cooling innovation has leveled off in recent years, as shown in **Figure 1**.

Since the 1970s, processor's raw power has increased leaps and bounds over its origins. However, over the years, as more power and functionality was packed into smaller chips, heat dissipation became more of an issue than ever before. In 1993, a private company, Arctic Silver, did introduce thermal paste to processors, which did a decent job at enhancing the rate of heat transport away from the chip. Moreover, this was applicable to both laptops and desktops, and today, tablets. Without thermal paste, computer processor clock speeds would be about .4-.5 GHz lower than they are now.

Unfortunately, since then, the thermal paste and the fan have been the mainstay for cooling. Almost every desktop and laptop computer built in the last 15 years has the same combination to cool processors. As processor speeds kept increasing, more efficient fans were developed, and the fans were run at a higher angular velocity, but eventually any opportunity for improvement in this design started to stagnate by the mid-2000s. By the year 2007, desktop clock speeds with a traditional cooler have plateaued at a constant 3.5 GHz, due to a lack of innovation in processor cooling. To qualify the aforementioned statement, water cooling was invented in 2004, which was decently effective at increasing the clock speeds of computers by as much as 1.0 GHz, but this solution was only applicable to desktops, as laptops and tablets simply do not have the space to house such a system.

Based on this information, there is a strong need to innovate in processor cooling technology to keep up with the pace of processor technology innovation.

Heat Transport and Carbon Nanotubes

In recent years, carbon nanotubes have become more of a mainstay in physical science research. This is partly due to their high tensile strength, electrical conductivity, and most importantly, thermal conductivity.

Carbon nanotubes are currently being developed to replace the thermal paste to increase the rate of heat transfer from the computer processor to the cooling fan and ambient air. This is because their Fermi-structure geometry enables them to conduct thermal energy longitudinally efficiency. For the raw transport of thermal energy, multi-walled carbon nanotubes are the most effective as they are vertically grown and include multiple layers, according to **Figure 2**. Thus, thermal energy can be directly dissipated from the mating surface. These types of carbon nanotubes, including the one performed in this research, are grown through a process known as Plasma Vapor Deposition, in which a substrate, most likely Silicon, is subject to extremely high temperatures and the bombardment of gaseous plasma polymers and a carbonic gas, such as ethaline or methane, whose reaction causes vertically

grown graphenic structures bonded to the silicon substrate.

However, due to the lack of the capability of MWCNTs being able to bond to other substances, much of the conduction capability of CNTs (about 3500 W/m-K) is lost due to high thermal interface resistance with the mating surface. This is not an effect on the materials of the two surfaces, but rather, the juncture in between. In most cases, the CNTs will adhere to mating metal surfaces, but only through a weak van-der-Waals force. This is due to the fact that the Fermi geometry of the nanotubes does not line up with the amorphous geometry of most metals, indicating a weak force, at best, or no force at all, at worst. While carbon nanotubes have proven to be moderately effective over thermal paste to cool processors, much of their capability is lost due to this phenomenon. In most research that was conducted with nanotubes cooling metallic mating surfaces, the average thermal conductivity of the juncture was only about 1000 W/m-k, which was significantly lower than CNT's inherent thermal transport conductivity of 3500 W/m-K.

Forcing Covalent CNT Bonding

Carbon nanotubes do not inherently bond with other substances. This is due to the natural bonding structure of the carbon nanotube and other strictly carbon substances. A double bond is formed with another carbon atom, and the two other bonds are single atoms. The double bond, in theory, could be broken up by an oxygen atom on one bond, but this cannot occur under other substances in standard temperature and pressure. **Figure 3** depicts the chemical structure of a carbon nanotube array, and why breaking up any of the C-C bonds is nearly impossible under normal adhesion.

However, in theory, a plasma treatment should be able to break up one of the π bonds of the double bonds between the two carbon atoms. This is done through the fact that trioxidane based radicals at high temperatures have an extremely high attractiveness factor to bonding, and have been known to split strong organic bonds. These high energy chemicals are attracted to the bond, effectively splitting it up and creating a methane reagent. In the end, the double bond is effectively split into two with the σ bond connecting the carbon atoms together and the π bond joining the graphene structure to the oxygen radical, which would later enable bonding to other substances, as being a heterogeneous compound. Last year's research confirmed this theory, in which an oxidized CNT array was able to covalently mate with aminopropyl triethoxysilane, and conducted thermally at a rate of 2736 J/m-K. The new oxidized structure is illustrated by **Figure 4**.

To summarize: the reaction occurs as follows (Graphene is assumed to be C_{12}):

$$8C_{12} + 10H_2O_3 + \Delta Q \longrightarrow 7C_{12}O_4 + 6C_2H_2 + 4H_2O \quad (2)$$

With the exhaust products being gaseous acetylene and water vapor. It is important to note that the aforementioned reaction can only occur at high temperature and low pressure, such a plasma. Vacuum reactions in the plasma etcher generate trioxidane radicals to allow bonding to take place at high temperatures.

Quantum Thermodynamics/Phonon Density of States

In quantum thermodynamics, thermal energy is transported through pulses in the form of phonons, or the frequential excitation of atoms. The optical frequency of these phonons is directly proportional to the thermal transport capability of the specific structure. Their superior electrical and thermal transport capability is determined by the location of the π bonds, which in Fermi structures such as carbon nanotubes and graphene, are exactly 12 eV apart. This arrangement forms wide electronic valence and conduction through the bonds. This aligns the mating bonds in the M-T-K directions, exactly 120 degrees apart from one another. This forms Dirac points between the bonds, around which the phonons get distributed in the shape of an equilateral triangle. A radially conical phonon cluster is thus formed around the Dirac points, and, due to their equilateral nature, can be easily transmitted from point to point at a higher frequency. This is also due to the fact that the π bond electronic dispersion is forced to be linear, which evenly matches up with the equilateral phonon field.

However, it is important to note that oxidized carbon nanotubes form weak ionic bonds with aluminum by default, but not strong covalent bonds. To bypass this apparent obstacle of heat transfer, a substrate with a Fermi bond structure can be introduced, such as various silanic substrates. In theory, the silane which would produce bonds closest to 12eV apart is Aminopropyl Triethoxysilane, or Si_2NH_4. This is from the mating of the valence orbitals that produces the bonds near the M-T-K directions, especially in the hydroperoxyl and trioxidane radicals that mate the substrate to the Aluminum surface of the processor. Moreover, the nitrogen atom forms two π bonds with carbon hydride radicals linking to the silanic substance. A final sigma bond, about 0.3eV off the T direction, links the nitrogen atom to the oxidized carbon nanotubes. To better get a grasp of this bond that is being functionalized between the MWCNTs and aluminum plate, please consult with **Figure 7**.

Fermi Diversion Levels

Fermi materials contain a five dimensional symplectic structure. These include three real space vectors (x, y, z) and two k-space vectors, neither of which is time. One of the k-space vectors is paired up with one of the real space vectors, and the remaining two real space vectors are paired up with each other. The remaining k-space vector is known as the Fermi-velocity direction. When looked at in relationship to the three-space, the fermi-velocity forms a logarithmically symmetrical gap at a perfectly equilateral Fermi diversion. In normal circumstances, the Fermi-velocity forms a logarithmic vector around the three-space and can be measured based on units of the gauge point density. The gauge point density, or GPD, is equal to the ration of an existent Fermi-velocity direction and a logarithmically symmetrical gradient. It is primarily used for calculating symmetricity of multidimensional particles and realistically provides a relationship for the vector angle between this direction and another direction. The equation

for the gauge point density, or GPD, is equal to the following:

$$D = \varphi + e^{32\pi\hat{}2} \ (3)$$

where φ is equal to the three-space gradient slope. Interestingly, in a perfectly symmetrical fermi-velocity vector, the GPD is equal to exactly 1, and is true only when the 3-space gradient slope is equal to $2\ln(\pi\sqrt{3}/2)$, which occurs in a perfectly equilateral triangle with a maximum eV diversion of 12.0. (Fermi level is based on a scale from 0.0 to 12.0, with 12.0 causing the least bottlenecks as equilateral phonon radials most efficiently disperse phonons off the Dirac points.

One main question that can be gained from such a phenomenon is whether or not quantum phonon theory can explain the relationships between 3-space Fermi diversion levels and the symmetricity (and effectiveness) of phonon transport. If such a question were to be true in a realistic application, then the relationship between the fermi diversion and contact success would be exponential.

Summary of Last Year's Experiment

Last year's experiment was to simply apply these principles on whether or not adding a covalently bonded organic substrate would increase the contact success and thus the thermal dissipation between an aluminum plate and carbon nanotubes, when compared to a simple van der Waals juncture. Since advanced laser pulse machines were unavailable to test, a more simple test bed was put in place, involving placing the juncture itself onto an electric resistance plate, which was the simulation of the processor itself.

The experiment was carried out for both a simple van der Waals juncture and a covalently bonded juncture with aminopropyl triethoxysilane, a highly symmetrical molecule used primarily to apply glass fibers to polymer matrices. Oxygen plasma etching was carried out on the MWCNT sheet to enable the oxidized CNTs to bond covalently with the aminopropyl triethoxysilane, which itself would bond to the aluminum surface. Fifteen trials were conducted for this experiment.

First, the temperature gradient, or dT/dY was calculated, based on the temperature differential between the silicon substrate and the nanotubes, and the distance between the two surfaces, in this case 0.4 mm. Using this, the contact success was calculated by modifying **Equation 4**, the formula for finding the contact success for graphene,

$$\sigma = dYe^{\sqrt{3}\times10^{-9}x} \ (4)$$

to a function of surface area, due to the fact that contact success is a function of area. The initial equation was simply manipulated to replicate the formula for surface area based on shells with a side length equal to the arc length of such a body:

$$\sigma_s = \int_0^{\pi\times1.0\times10^{-7}} \sigma\sqrt{1+(\frac{d\sigma}{dx})^2}\ dx \ (5)$$

The indefinite integral is graphed in **Figure 5**, which shows contact success as a function of temperature gradient.

The contact success obtained from the function can then be used to calculate the actual conductivity of the junctures, by multiplying the decimal form of the contact success by the maximum conductivity of a perfectly flawless graphene array. As shown in **Figure 6**, the juncture functionalized by the aminopropyl triethoxysilane had a thermal conductivity of 2736 W/m-K, or 2.68 times higher than the simple van der Waals juncture, which had a conductivity of only 1026 W/m-K. The main takeaway from this project is stated below in italics:

While CNTs alone have a supremely high phonon optical frequency and transport rate, their capacity is not put to good use, due to high thermal interface resistance and low contact success between the CNTs and the mating surface. However, more efficient bonds can be formed between the two materials to drastically increase phonon frequency and thermal transport rates.

Premise of Project

Based on last year's research, it is known that adding a symmetrical substrate into a CNT juncture, when in contact with a mating surface, drastically increases the thermal dissipation and contact success. However, that is only half of the story. Materials such as aminopropyl triethoxysilane, which contain nearly perfectly equilateral molecules, are expensive to produce, and it is possible that slightly less ordered molecules may not lose a lot of contact success from a perfect juncture.

The purpose of this project is to develop a relationship that engineers can use when determining what substrate can be used to bond to MWCNT array for maximum contact success in several applications, including the cooling of laptop and tablet processors. Side effects from this study will include calculating the actual contact success of individual molecules, and how much a minute change in the Fermi diversion, or cost, would affect the contact success, or conductivity, of the juncture.

Experiment

Design Brief

Problem Statement: *What relationship exists between Fermi diversion level of substrates and the contact success of dissimilar materials, for example Multiwalled carbon nanotubes and metallic surfaces?*

Hypothesis: *If three organic compounds, each with varying 3-space molecular geometry (and thus varying Fermi diversion) are applied to a plasma-etched CNT array, then the contact success will be equal to the natural exponential function of the Fermi diversion.*

The basis behind the hypothesis is that the K-space phonon theory is valid in this application, because when the gauge point density, or GPD, equals one, the fermi velocity will be in a direction logarithmically proportionate to the 3-space.

Materials Used

Perhaps the most important materials used for the experiment were the chemicals, which are aminopropyl triethoxysilane, hydroxylsilane hydrochloride, and methyl-2-silicoacrylate. Aminopropyl triethoxysilane (**Figure 8**) is commonly used to apply glass fibers to polymer matrices, especially in the treatment of window casements. Hydroxylsilane hydrochloride is used as a vulcanization accelerator in the rubber industry, and commonly used for gaskets and filling cracks and leaks in various structures. Methyl-2-silicoacrylate is used for instant glues, and are known for fast curing yet being brittle. Interestingly, all three organic substrates bond the aluminum directly with the Si-H bonds, but it is the bonds between this sub-molecule and the oxidized MWCNT that determines the Fermi level of the juncture. **Figure 7** depicts the chemical structure.

Other materials required were four 1 cm square MWCNT sheets (**Figure 9**) grown on Silicon substrate. This process was done at NanCyl tubes, a laboratory in Vermont. The researcher was unable to enter the room during the plasma vapor deposition, due to high temperature and inhaling hazards. Four 1 cm square aluminum plates were also required as the simulation for the processor plate.

A plasma etcher served as the means of oxidizing the MWCNTs to enable them to bond covalently. Other materials included a plasma etcher, thermometer probe (**Figure 10**), copper resistance plate (**Figure 11**, the heat source), syringe, 9V battery, paintbrush, gloves, and a ruler.

Experimental Procedure

To ensure safety during various parts of the experiment, safety gloves were worn when conducting all aspects of the experiment. In addition, aminopropyl triethoxysilane is flammable, and its chemical adhesion had to take place under a range hood until the bond fully cured, in which it was safe to remove and perform experimentation. In addition, the house temperature was set to a constant, 22.2°C, to maintain accuracy on the data. The entire experiment was conducted in a house, except the plasma etching, which took place at Lehigh University's Materials Science Laboratory.

As shown in **Figure 12**, the battery was connected to the copper resistance plate on top of a Styrofoam test-bed, to reduce any unintentional movements and variations in the data. The temperature of the resistance plate was measured until it reached a constant, which would become the juncture temperature of the trial. One of the CNT sheets was then placed on one of the aluminum plates, with strong adhesion in a van der Waals juncture. This plate was then placed on top of the copper resistance plate, as shown in **Figure 13**, and the distance between the two was measured using a metric ruler, which was 0.4 mm. After this, the temperature of the top of the CNT juncture was measured until it reached a constant. This entire process for the control group was repeated fifteen times for added accuracy.

For the functionalized juncture, or the control group, oxygen plasma etching (**Figure 14**) was applied to the CNT sheet, 4 cm above the MWCNT array. This would inject high energy trioxidane radicals that would break up one of the pi ponds of the CNT array, thus making covalent bonding possible. Next, a syringe was used to apply 0.5 mL of the aminopropyl triethoxysilane to one of the unused aluminum plates in a ventilated area. The CNT sheet was then directly placed on top of the aluminum plate, creating the full functionalized juncture.

The rest of the steps for testing the aminopropyl triethoxysilane would be the same as with the van der Waals juncture. The entire experiment was then repeated for the other two chemicals, hydroxylsilane hydrochloride and methyl-2-silicoarylate, using the plasma etcher to form covalent bonds.

Experimental Variables

The manipulated variable was the Fermi geometry between the aluminum plate and the CNT sheet, which was based on the substrates themselves. The responding variable was the contact success of the juncture, which was later calculated using integration of the temperature gradient.

Three controlled variables of the experiment were the ambient temperature (22.2°C), the heat generated by the copper plate, and the thickness of the grown MWCNTs, which was 100nm.

Analysis

Figure 15 shows the measured temperatures at the junction and substrate for the van der Waals juncture. The average temperature differential between the two locations was 8.6°C. **Figure 16** shows the measured temperatures at the junction and substrate for the aminopropyl triethoxysilane juncture. The average temperature differential between the

two locations was 3.4°C. **Figure 17** shows the measured temperatures at the junction and substrate for the hydroxylsilane hydrochloride juncture. The average temperature differential between the two locations was 6.0°C. **Figure 18** shows the measured temperatures at the junction and substrate for the methyl-2-silicoacrylate juncture. The average temperature differential between the two locations was 4.1°C. Note that the van der Waals juncture had the largest temperature differential and the aminopropyl triethoxysilane juncture had the lowest temperature differential.

Based on the temperature differentials, the temperature gradient, or dT/dY was calculated, in which dY, or the distance between the resistance plate and top of the CNT juncture was 0.4 mm. **Figure 19** shows that the van der Waals juncture had a temperature gradient of -21675 K/m, the aminopropyl triethoxysilane juncture had a temperature gradient of -8127 K/m, the hydroxylsilane hydrochloride had a temperature gradient of -15000 K/m, and the methyl-2-silicoacrylate had a temperature gradient of -10250 K/m. A higher temperature gradient indicates that the particular substrate was more of an insulator than a conductor, as much of the heat in the van der Waals juncture was bottlenecked by high thermal interface resistance towards the carbon nanotubes. On the other hand, the aminopropyl triethoxysilane was the most conductive, since it had the lowest temperature gradient.

To generate the actual relationship, the Fermi diversions and contact success had to be calculated. The Fermi diversions are calculated by **Equation 6**:

$$D(f) = \frac{12}{e^{(E-E_f)/kT}+1} \quad (6)$$

where E = bond energy level with the oxidized CNT, E_f = the energy level of the highest Fermi level, and kT is the thermal energy in the bonds. From this, the van der Waals juncture had a Fermi level of 9.75 eV, the aminopropyl triethoxysilane had a Fermi level of 11.51 eV, the hydroxylsilane hydrochloride had a Fermi level of 10.18 eV, and the methyl-2-silicoacrylate had a Fermi level of 10.79 eV. This is a material property of the substrates, and a higher Fermi level indicates higher symmetricity.

The contact success was calculated by modifying the contact success function for a 2D graphene structure in **Equation 4:**

$$\sigma = dYe^{\sqrt{3}\times10^{-9}x} \quad (4)$$

to a function of surface area, due to the fact that contact success is a function of area. The initial equation was simply manipulated to replicate the formula for surface area based on shells with a side length equal to the arc length of such a body:

$$\sigma_s = \int_0^{\pi\times1.0\times10^{-7}} \sigma\sqrt{1+(\frac{d\sigma}{dx})^2}\ dx \quad (5)$$

Based on this calculation, the van der Waals juncture had a contact success of 0.351, the aminopropyl triethoxysilane had a contact success of 0.719, the hydroxylsilane hydrochloride had a contact success of 0.407, and the methyl-2-silicoacrylate had a contact success of 0.483. It seems apparent that the contact success is positively correlated with the Fermi geometry of the substrates, but it is only when these points are plotted when an actual relationship can be determined.

Figure 20 displays the four curves on a x-y scatter plot with contact success as a function of Fermi diversion. The initial, hypothesized relationship, $y = e^{x-12}$, is in grey, while the trend line with least residual values is in orange. This orange line had an equation of:

$$y = 0.8684e^{x-12} + 0.1298 \quad (7)$$

which, when looked closely, is equal to the following equation (**Equation 1**):

$$y = \frac{\sqrt{3}}{2}e^{x-12} + (1-\frac{\sqrt{3}}{2}) \quad (1)$$

Note how the actual relationship is higher and does not decrease as exponentially as the hypothesized relationship, and that it levels out at an asymptote above y = 0.

To verify that this was indeed the actual relationship, a statistical analysis was performed on the linearization of **Equation 1**, as shown in **Figure 21**. Since the R^2 coefficient is greater than 0.95 (0.9869 to be exact), valid conclusions can be drawn that this **Equation 1** fact is the relationship.

Conclusion

Hypothesis Analysis

Hypothesis: *If three organic compounds, each with varying 3-space molecular geometry (and thus varying Fermi diversion) are applied to a plasma-etched CNT array, then the contact success will be equal to the natural exponential function of the Fermi diversion.*

The initial hypothesis is partially supported. According to **Figure 20**, the actual trend line of the relationship was significantly higher than the hypothesized relationship, and was equal to **Equation 1**, or

$$y = \frac{\sqrt{3}}{2}e^{x-12} + (1 - \frac{\sqrt{3}}{2}) \quad (1)$$

It is very likely that the added coefficients stem from the geometry of the CNT interface, since graphene structures form equilateral Fermi bonds with sp^2 hybridization. The ratio of $\sqrt{3}/2$ is commonly seen in equilateral triangles as the ratio of the hypotenuse vector length to the leg vector length. An explanation for the y intercept of $1-\sqrt{3}/2$ is that even when two surfaces mate without any contact, i.e. adhesive forces, phonons can still be transported between the two materials. An example for this is touching a finger on a cold water faucet.

Another interesting find is that the contact success did not decrease as quickly as initially hypothesized, partly due to the decreased slope caused by the added coefficients. Nevertheless, the contact success does still decrease exponentially before leveling off at an asymptote. A small decrease in the symmetricity will still have a large impact on the contact success and conductivity of the juncture.

Nevertheless, based on the findings in this experiment, the 5-Space Quantum Theory can explain relationships between Fermi Diversion levels and symmetricity of phonon transport.

Errors and Fixations

A possible source of error in this experiment is that the temperature gradient vertical differential, or dY, was measured using a ruler, and a magnifying glass was used to estimate the factor in between the marked millimeter bars. A way that this problem can be redeemed is by using a SONAR sensor to measure the distance from the resistance plate to the silicon substrate.

Practical Application

Based on last year's research, it is known that adding a symmetrical substrate into a CNT juncture, when in contact with a mating surface, drastically increases the thermal dissipation and contact success. However, that is only half of the story. As shown in the experiment, the thermal conductivity rapidly decreases with a small de-symmetricalization of a juncture's chemistry. High conductivity only occurs at very high Fermi diversions.

The purpose of this project is to develop a relationship that engineers can use when determining what substrate can be used to bond to MWCNT array for maximum contact success in several applications, including the cooling of laptop and tablet processors. Side effects from this study include calculating the actual contact success of individual molecules, and how much a minute change in the Fermi diversion, or cost, would affect the contact success, or conductivity, of the juncture.

Future Study

In the future, an experiment can be tested on how much the clock speed of a processor can be increased without damage when using a Fermi CNT cooler and with just a standard CNT cooler mated through the van der Waals force. Also, different silanic substances can be tested on the effect of CPU clock speed and thermal transport rate. This is all dependent on the geometry of the π bonds in the materials, which ultimately yields to the equilarity of the phonon radials. This is likely going to be a future extension to this experiment as the exact geometry of the phonon radials can be compared more efficiently with one another.

Finally, CNT heatsinks do not only have to be applied to CPUs. There are several applications in which a large amount of heat has to be dissipated to maintain integrity in the original structure. One example is rocket nozzles, which, from friction of exploding gas, have a likelihood to have a very high temperature. These materials are also made of ceramic, which are good insulators, but not conductors. A CNT heatsink can be effectively added to such a system to increase thermal dissipation. Another application is in a fusion chamber, in which high thermal energy is released from radioactive chemicals. To eliminate the potential of heat further altering the chemicals, CNT heatsinks are vital to allow smooth heat transport between the two surfaces.

Acknowledgements and References

Acknowledgements:

- Shunqiang Wang of Lehigh University (Ph.D. Student), and Dr. Liu of Lehigh University (Materials Science Professor) for availability of Plasma Etcher to use, along with safety procedures for their usage.
- NanCyl Tubes of Vermont was willing to send a small CNT sample that was used in this experiment. This was custom made to request, using Plasma Vapor Deposition.

References:

Ago, H. et al. Work functions and surface functional groups of multiwallcarbon nanotubes. J. Phys. Chem. B 103, 8116–8121 (1999)

Antonelli, G. A., Perrin, B., Daly, B. C. & Cahill, D. G. Characterization ofmechanical and thermal properties using ultrafast optical metrology. MRS Bull.31, 607–613 (2006)

Cola, A. B., Xu, J. & Fisher, T. S. Contact mechanics and thermal conductanceof carbon nanotube array interfaces. Int. J. Heat. Mass. Tran. 52, 3490–3503(2009).

Hu, M., Keblinski, P., Wang, J.-S. & Raravikar, N. Interfacial thermalconductance between silicon and a vertical carbon nanotube. J. Appl. Phys. 104,0835031 (2008).

Hu, X. J., Padilla, A. A., Xu, J., Fisher, T. S. & Goodson, K. E. 3-omegameasurements of vertically oriented carbon nanotubes on silicon. J. Heat.Trans. T. Asme 128, 1109–1113 (2006)

Hu, X. J., Panzer, M. A. & Goodson, K. E. Infrared microscopy thermalcharacterization of opposing carbon nanotube arrays. J. Heat. Trans-T. A sme129, 91–93 (2007)

Kraemer, D. et al. High-performance flat-panel solar thermoelectric generatorswith high thermal concentration. Nat. Mater. 10, 532–538 (2011)

Krishnan, S., Garimella, S. V., Chrysler, G. M. & Mahajan, R. V. Towards athermal Moore's law. IEEE. T. Compon. Pack. T 30, 462–474 (2007)

Losego, M. D., Grady, M. E., Sottos, N. R., Cahill, D. G. & Braun, P. V. Effects ofchemical bonding on heat transport across interfaces. Nat. Mater. 11, 502–506(2012)

Pop, E., Mann, D. A., Goodson, K. E. & Dai, H. Electrical and thermal transportin metallic single-wall carbon nanotubes on insulating substrates. J. Appl. Phys.101, 093710 (2007)

Prasher, R. Acoustic mismatch model for thermal contact resistance of van derWaals contacts. Appl. Phys. Lett. 94, 041905 (2009). 20. Cahill, D. G. Analysis of heat flow in layered structures for time-domainthermoreflectance. Rev. Sci. Instrum. 75, 5119 (2004)

Prasher, R. et al. Nano and micro technology-based next-generation package-level cooling solutions. Intel Technol. J. 9, 1571 (2005)

Prasher, R. Thermal boundary resistance and thermal conductivity ofmultiwalled carbon nanotubes. Phys. Rev. B 77, 075424 (2008)

Prasher, R., Tong, T. & Majumdar, A. An acoustic and dimensional mismatchmodel for thermal boundary conductance between a vertical mesoscopicnanowire/nanotube and a bulk substrate. J. Appl. Phys. 102, 104312 (2007)

Samson, E. C. et al. 'Interface material selection and a thermal managementtechnique in second-generation platforms built on intel centrino mobiletechnology'. Intel Technol. J. 9, 75 (2005)

Schmidt, A., Chiesa, M., Chen, X. & Chen, G. An optical pump-probetechnique for measuring the thermal conductivity of liquids. Rev. Sci. Instrum.79, 064902 (2008)

Wang, Z. L., Li, Q. & Tang, D. W. Experimental Reconstruction of ThermalParameters in CNT Array Multilayer Structure. Int. J. Thermophys. 32,1013–1024 (2011)

Yu, M., Funke, H. H., Falconer, J. L. & Noble, R. D. High density, vertically-aligned carbon nanotube membranes. Nano Lett. 9, 225–229 (2009)

Equations

1) $y = \frac{\sqrt{3}}{2}e^{x-12} + (1 - \frac{\sqrt{3}}{2})$ (Developed Relationship of Contact Success v. Fermi Diversion)
2) $8C_{12} + 10H_2O_3 + \Delta Q \longrightarrow 7C_{12}O_4 + 6C_2H_2 + 4H_2O$ (Plasma Etching of MWCNTs)
3) $D = \varphi + e^{32\pi\text{^}2}$ (Gauge Point Density)
4) $\sigma = dYe^{\sqrt{3}\times10^{-9}x}$ (Contact Success of 2D Graphene Array)
5) $\sigma_s = \int_0^{\pi\times1.0\times10^{-7}} \sigma\sqrt{1 + (\frac{d\sigma}{dx})^2}\ dx$ (Contact Success for 3-D Graphene Array)
6) $D(f) = \frac{12}{e^{(E-E_f)/kT}+1}$ (Fermi Diversion Level)
7) $y = 0.8684e^{x-12} + 0.1298$ (Trend Line of Relationship)

Figures

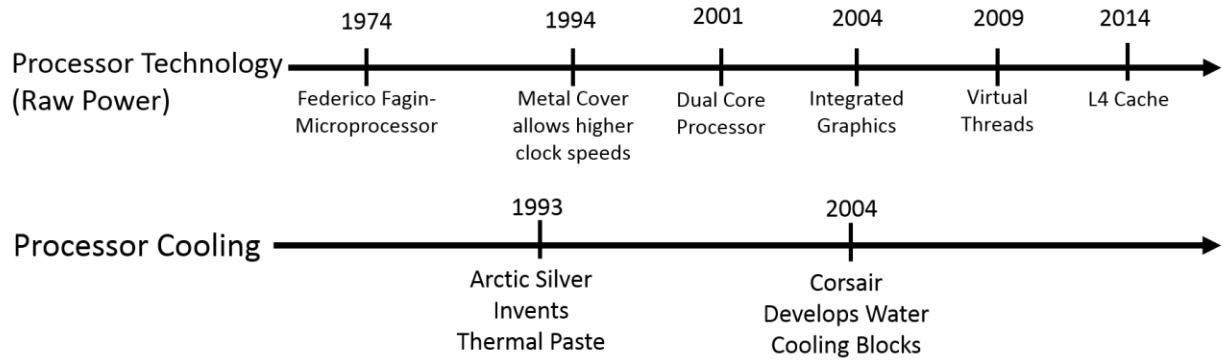

Figure 1: Processors Innovation Timeline

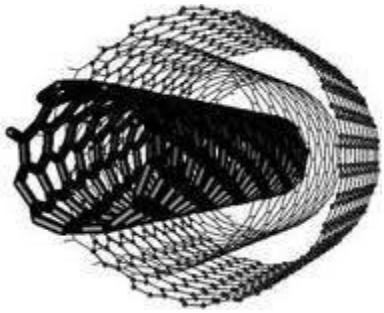

Figure 2: MWCNT Cross Section

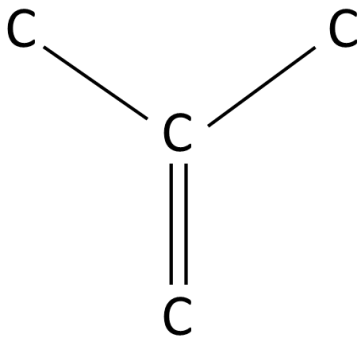

Figure 3: Graphene Structure

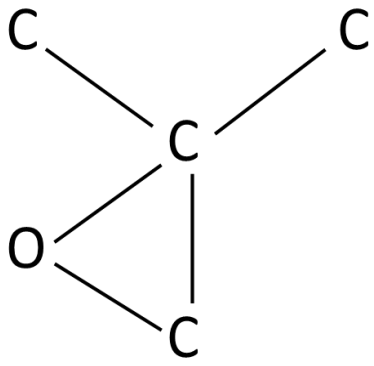

Figure 4: Chemical Structure of oxidized MWCNTs

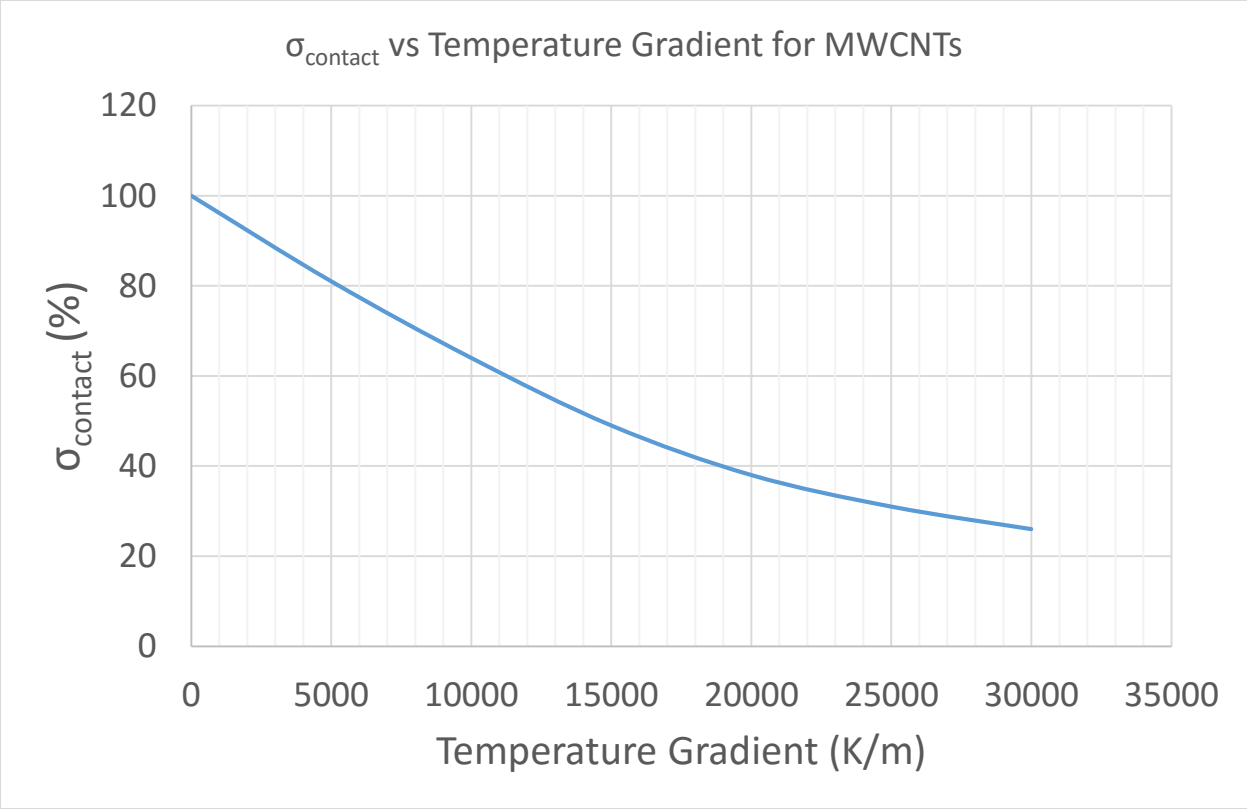

Figure 5: Contact Success as a function of Temperature Gradient

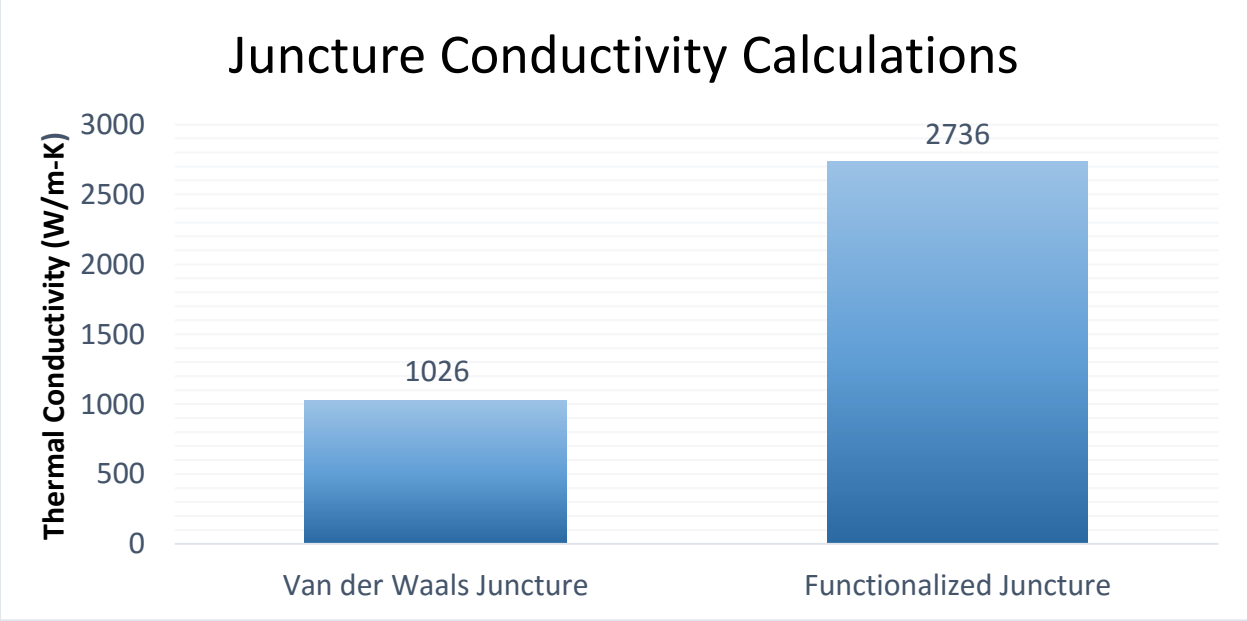

Figure 6: Conductivities of Junctures

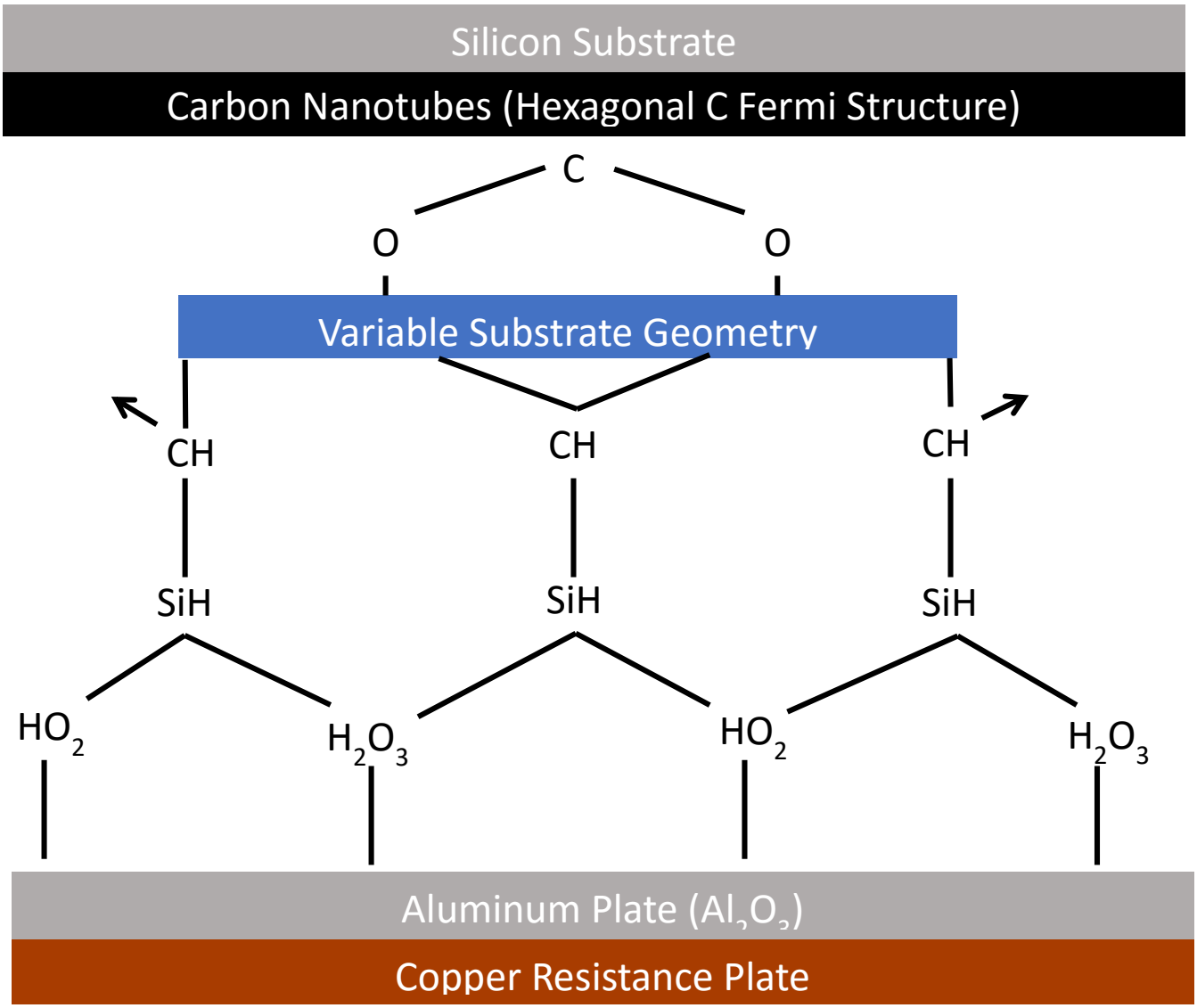

Figure 7: Functionalized Juncture Diagram

Figure 8: Aminopropyl Triethoxysilane

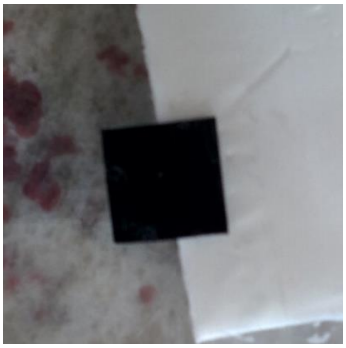

Figure 9: CNT Array

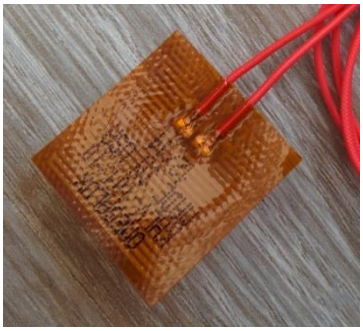

Figure 10: Copper Resistance Plate

Figure 11: Thermometer Probe

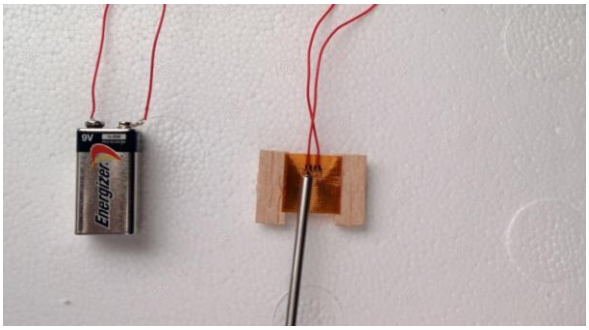

Figure 12: Measurement of Junction Temperature

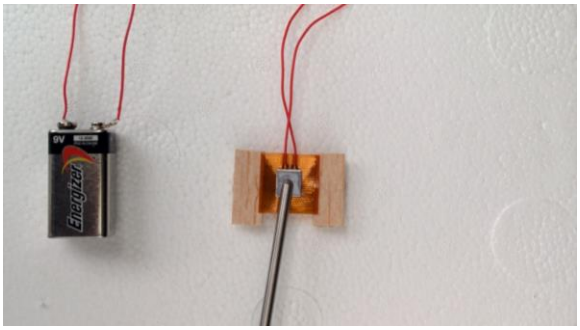

Figure 13: Measurement of Substrate Temperature

Figure 14: Plasma Etching

TRIAL	Junction Temperature (°C) (Hot Plate)	Substrate Temperature (°C) (Top of Nanotube Substrate)
1	54.2	44.1
2	51.7	44.4
3	51.6	42.7
4	51.4	42.3
5	51.7	42.5
6	51.9	42.8
7	51.3	43.0
8	50.9	44.5
9	52.1	44.9
10	51.5	43.1
11	51.7	42.7
12	51.6	44.4
13	51.4	42.3
14	52.3	41.9
15	52.0	41.7
MEAN	**51.8**	**43.2**

Figure 15: Temperature Recordings for van der Waals Juncture

TRIAL	Junction Temperature (°C) (Hot Plate)	Substrate Temperature (°C) (Top of Nanotube Substrate)
1	55.2	51.7
2	52.3	49.3
3	53.7	50.5
4	53.9	49.7
5	53.2	50.0
6	52.1	51.6
7	55.0	49.2
8	52.2	50.4
9	54.0	49.6
10	53.9	49.8
11	53.2	52.0
12	55.4	49.5
13	52.5	50.7
14	53.7	49.8
15	52.9	50.1
MEAN	**53.6**	**50.2**

Figure 16: Temperature Recordings for aminopropyl triethoxysilane juncture

TRIAL	Junction Temperature (°C) (Hot Plate)	Substrate Temperature (°C) (Top of Nanotube Substrate)
1	53.6	45.6
2	52.7	47.1
3	53.3	46.1
4	53.7	46.2
5	51.3	47.0
6	53.9	47.1
7	52.1	46.8
8	51.8	46.3
9	51.5	46.4
10	53.1	45.4
11	52.9	47.8
12	51.4	47.1
13	53.6	47.6
14	52.1	45.9
15	52.2	46.1
MEAN	**52.6**	**46.6**

Figure 17: Hydroxylsilane Hydrochloride Juncture temperature calculations

TRIAL	Junction Temperature (°C) (Hot Plate)	Substrate Temperature (°C) (Top of Nanotube Substrate)
1	50.4	46.3
2	50.7	46.2
3	51.1	46.6
4	50.4	45.9
5	51.5	47.1
6	52.1	48.1
7	50.8	47.5
8	50.3	46.2
9	51.6	47.4
10	51.7	47.3
11	53.1	48.9
12	52.4	48.2
13	51.8	47.9
14	50.2	46.5
15	50.4	46.2
MEAN	**51.2**	**47.1**

Figure 18: Methyl-2-Silicoacrylate Juncture Temperature Calculations

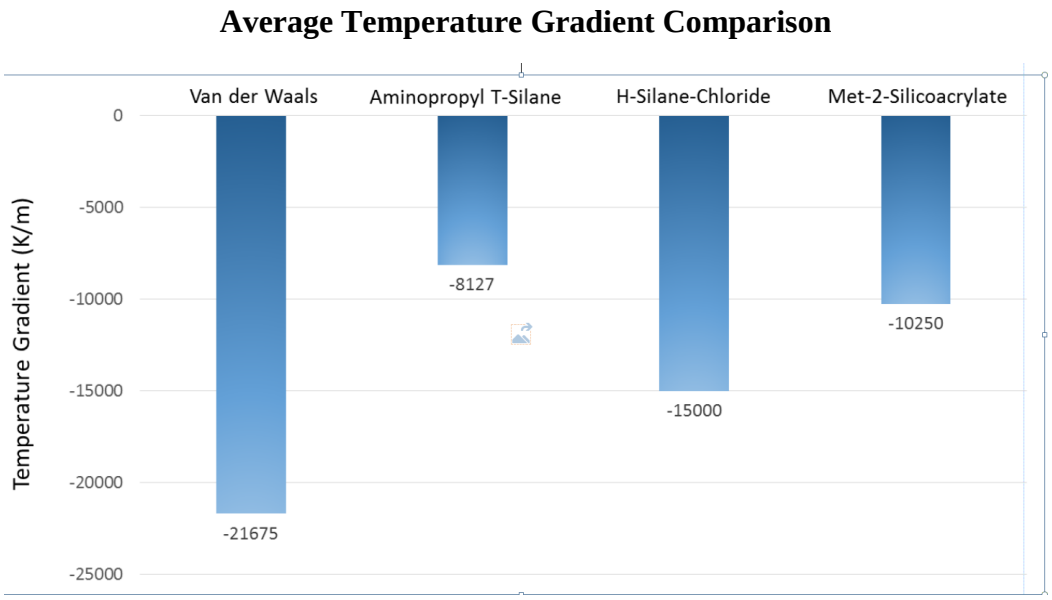

Figure 19: Average Temperature Gradient Comparison

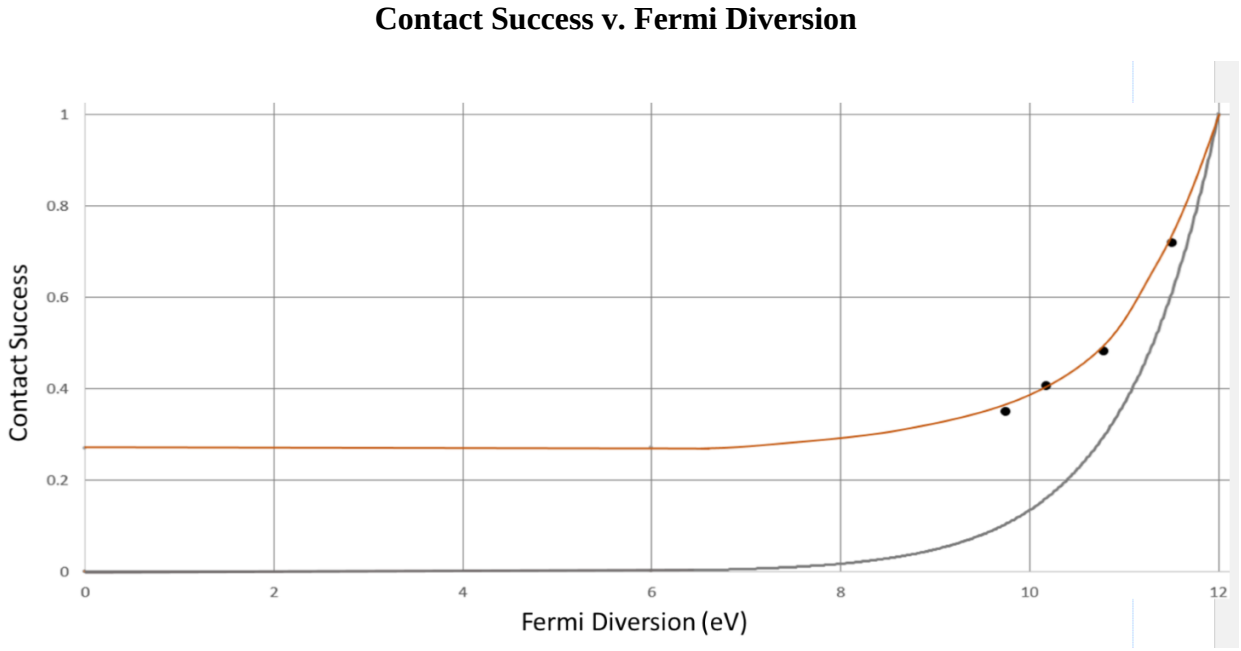

Figure 20: Contact Success v. Fermi Diversion (Grey curve = hypothesized curve, Orange curve = trend line curve)

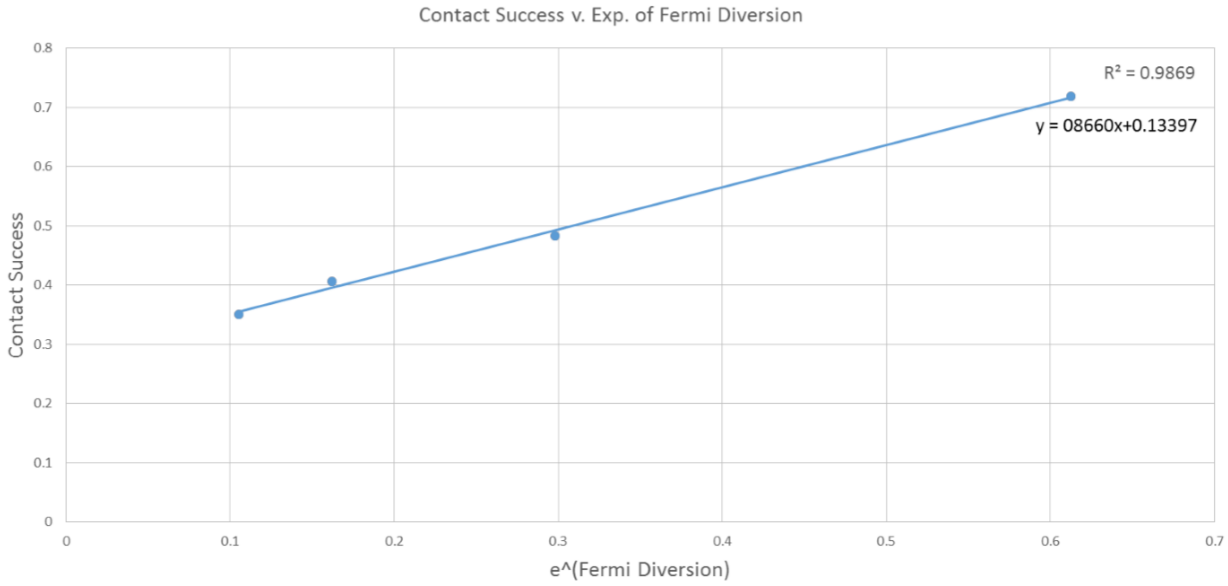

Figure 21 Contact Success v. Exponential function of Fermi Diversion